Eighth South African Conference on Computational and Applied Mechanics
SACAM2012
Johannesburg, South Africa, 3−5 September 2012

Strongly Coupled Partitioned FSI Using Proper Orthogonal Decomposition

AEJ Bogaers*, S Kok†, T Franz‡§¶‖
*†Advanced Mathematical Modelling, CSIR Modelling and Digital Science, South Africa
*Email: abogaers@csir.co.za
‡Cardiovascular Research Unit, Chris Barnard Division of Cardiothoracic Surgery, UCT, South Africa
§Centre for Research in Computational and Applied Mechanics, UCT, South Africa
¶Programme for the Enhancement of Research Capacity, Research Office, UCT, South Africa
‖Centre for High Performance Computing, Rosebank, South Africa

***Abstract*—In this paper we present a strong coupling algorithm for partitioned fluid-structure interactions which can be applied to black-box field solvers. The coupling algorithm constructs an approximate interface Jacobian of the coupled fluid-structure problem using proper orthogonal decomposition (POD) reduced order models of the interface tractions and displacements. The coupling scheme is an augmentation of the IBQN-LS (interface block-quasi-Newton with an approximation for the Jacobian from least-squares) coupling scheme.**

The performance of the original IBQN-LS method is strongly governed by the number of previous time step histories that are retained, where there exists a problem specific optimal choice. In this paper we will demonstrate that this dependence on the number of retained histories is due to a trade off between increasingly ill-conditioned interface Jacobian, when too many histories are retained, and sub-optimal coupling convergence rates due to a loss of information when histories are discarded.

We will show that the POD augmentation allows for the re-use of all observations from previous time steps by limiting the matrix ill-conditioning while essentially retaining 'all' the information. Retaining all histories improves the approximation of the interface block-Newton Jacobian, which in turn improves the coupling iterations' convergence rates. We will demonstrate on a flexible tube benchmark problem that once sufficient information has been captured that the POD interface reduced order model can produce near quadratic convergence rates.

***Keywords*—Fluid-structure interactions; partitioned; approximate interface Jacobian; proper orthogonal decomposition**

I. Introduction

Fluid-structure interaction (FSI) has received a lot of attention in recent years within the biomedical field. Due to the incompressibility of the fluid and the close density ratios between the fluid and solid domains common in biomedical applications, a strongly coupled FSI code is necessary. There are two predominant solution methodologies, namely a monolithic solver or a partitioned solver with a strong interface coupling algorithm. Monolithic solvers solve all equations pertaining to the solid and fluid domains as well as the interface simultaneously. They do however require a large initial investment in terms of solver development. Partitioned solvers on the other hand employ pre-existing structural and fluid solvers and solve the two domains in a staggered fashion towards convergence. Of particular interest are those algorithms that treat each of the respective field solvers as "black-boxes".

One of the more promising "black-box" partitioned coupling schemes is the 'Interface Block Quasi-Newton with an approximation for the Jacobian from Least Squares Models' (IBQN-LS) scheme introduced by Vierendeels et al. [1]. The coupling scheme requires no access to either solver, and builds up an approximate interface Jacobian based only on historical observations of both the fluid tractions imposed on the interface surface and the boundary deformation of the interface based on these tractions. The method has been applied successfully to strongly coupled FSI problems, outperforming Aitken's relaxation method and compares favourably to interface-GMRES [2] and interface artificial compressibility [3]. Degroote et al. have also demonstrated how a similar reduced order modelling (ROM) based coupling scheme IQN-LS (Interface quasi-Newton with inverse Jacobian from a least squares model) ranges between 1/2 to 4 times the required computational cost of a full monolithic solver for a series of benchmark problems [4].

The original authors of the IBQN-LS coupling scheme have demonstrated that the number of time histories to be retained for the construction of the interface reduced order models (ROM) are problem dependent. However, in this paper we demonstrate that for a certain class of problems all the histories are important and should be retained. The perceived dependence on the number of retained time histories is as a result of increasing ill-conditioning of the ROM least squares (LS) matrices.

To this end, we introduce a minor augmentation of the original IBQN-LS method based on proper orthogonal decomposition (IBQN-POD). Proper orthogonal decomposition (POD) forms the optimal linear decomposition of any given set of system observations. If all the histories are retained, and the approximate Jacobian remains well conditioned, POD offers no additional advantage over the original least squares solution of the histories. It does however provide a mathematically quantifiable way in which information can be truncated such that the solution matrices remain well conditioned, while essentially retaining all the information.

II. Partitioned coupling algorithms

For most aero-elastic problems (for example flutter prediction of an aircraft wing), weak coupling is often sufficient, i.e. where a single fluid and solid computation suffices (often with no convergence check). These type of problems are usually characterized with fluid to solid density ratios $\frac{\rho_s}{\rho_f} > 1000$.

For problems in biomedics however the flow is internal with density ratios much closer to 1; this in addition to the incompressibility of the fluid flow leads to increased numerical effort. This phenomenon has been coined the 'added mass effect' [5], [6], where the solid deformation is often over predicted leading to potentially severe instabilities when employing a staggered solution scheme. Problems of this nature require the use of a strong-coupling algorithm, which in some way iterates on the boundary displacement until convergence.

A. Coupled FSI problem

In this paper we will focus only on FSI coupling using "black-box" field solvers. Each of the field solvers operate independently on non-overlapping fluid and structural domains Ω^F and Ω^S which share a common interface Γ. We denote each of the respective field solvers as interface operators which map interface displacements and forces. The solid solver is therefore an interface operator $\boldsymbol{S}$ that maps a given interface traction vector $\boldsymbol{f}_\Gamma^{n+1}$ to interface displacements

$$\boldsymbol{d}_\Gamma^{S,n+1} = \boldsymbol{S}_\Gamma \left(\boldsymbol{f}_\Gamma^{F,n+1} \right) \tag{1}$$

where the interface boundary is denoted by Γ, and $\boldsymbol{d}_\Gamma^{n+1}$ is the interface displacement vector at time step $n+1$. Similarly, the fluid field solver is represented by $\boldsymbol{F}$ such that

$$\boldsymbol{f}_\Gamma^{F,n+1} = \boldsymbol{F}_\Gamma \left(\boldsymbol{d}_\Gamma^{S,n+1} \right). \tag{2}$$

The fluid field operator $\boldsymbol{F}$ denotes both the solution step of the fluid field variables as well as the mesh movement of the fluid domain nodal coordinates.

For the FSI problem it is essential that both the kinematic and dynamic continuity is satisfied at all times. In the case of no-slip boundary conditions on the moving interface the kinematic continuity states that the fluid flow velocity at the interface $\boldsymbol{u}_\Gamma$ equals the boundary velocity

$$\boldsymbol{u}_\Gamma = \frac{\partial \boldsymbol{d}_\Gamma}{\partial t} \tag{3}$$

and dynamic continuity states that the traction forces are equal at the interface,

$$\boldsymbol{f}_\Gamma^S \cdot \boldsymbol{n} = \boldsymbol{f}_\Gamma^F \cdot \boldsymbol{n} \tag{4}$$

where $\boldsymbol{n}$ is the respective interface normals.

B. Fixed Point Iterations

Fixed point iteration schemes have gained a lot of popularity due to their simplicity and have proven to be robust for a large range of aero-elastic problems. The main idea of fixed point iteration schemes is to iterate back and forth between the two respective field solvers until the change in displacement updates fall below some specified tolerance.

Given that the FSI problem requires satisfaction of an interface equilibrium condition of

$$\boldsymbol{f}_\Gamma^{F,n+1} = \boldsymbol{f}_\Gamma^{S,n+1}, \tag{5}$$

it implies that an approximation to the interface displacement $\boldsymbol{d}_{\Gamma,k+1}^{n+1}$may be obtained by

$$\boldsymbol{d}_{\Gamma,k+1}^{n+1} = \boldsymbol{S}_\Gamma \left(\boldsymbol{F}_\Gamma \left(\boldsymbol{d}_{\Gamma,k}^{n+1} \right) \right), \tag{6}$$

The fixed point iteration scheme then iterates on the field operators until the interface displacement residual drops below some given tolerance ϵ where the time step residual is defined by

$$\boldsymbol{r}_{\Gamma,k+1}^{n+1} = \boldsymbol{d}_{\Gamma,k+1}^{n+1} - \boldsymbol{d}_{\Gamma,k}^{n+1}, \tag{7}$$

and k denotes the time step coupling iteration count.

The convergence stability of fixed point iterations can be augmented by including a relaxation factor ω_k such that

$$\boldsymbol{d}_{\Gamma,k+1}^{n+1} = \boldsymbol{d}_{\Gamma,k}^{n+1} + \omega_i \boldsymbol{r}_{\Gamma,k+1}^{n+1}. \tag{8}$$

However, for the class of problems encountered in biomedical problems, fixed point iterations with a constant relaxation parameter remain insufficient to guarantee convergence.

To this end, Aitken's Δ^2 dynamic relaxation [7], which can be likened to a secant method for vectors, is a useful augmentation to the fixed point relaxation iterations. The overall computational cost for strongly coupled aero-elastic problems are very competitive; it facilitates the use of "black-box" field solvers and has no additional overhead costs. Aitken's method recursively modifies ω based on

$$\omega^{k+1} = -\omega^k \frac{\left(\boldsymbol{r}^k\right)^T \left(\boldsymbol{r}^{k+1} - \boldsymbol{r}^k\right)}{\left(\boldsymbol{r}^{k+1} - \boldsymbol{r}^k\right)^T \left(\boldsymbol{r}^{k+1} - \boldsymbol{r}^k\right)}. \tag{9}$$

C. IBQN-LS

IBQN-LS (Interface Block Quasi-Newton with an approximation for the Jacobian from Least-Squares model), is a "black-box" coupling scheme introduced by Vierendeels et al. [1]. The scheme attempts to solve the FSI problem with block-Newton-Raphson iterations where the interface Jacobian is approximated via a least squares (LS) reduced order model (ROM).

If the FSI coupling problem is written as the following root finding problem

$$\boldsymbol{f}_\Gamma - \boldsymbol{F}\left(\boldsymbol{d}_\Gamma\right) = \boldsymbol{0} \tag{10}$$

$$\boldsymbol{d}_\Gamma - \boldsymbol{S}\left(\boldsymbol{f}_\Gamma\right) = \boldsymbol{0} \tag{11}$$

then the system can be solved by a block-Newton-Raphson iterative scheme where the linear system is expressed as

$$\begin{bmatrix} \boldsymbol{I} - \frac{\partial \boldsymbol{S}}{\partial \boldsymbol{d}_\Gamma} & \frac{\partial \boldsymbol{S}}{\partial \boldsymbol{f}_\Gamma} \\ \frac{\partial \boldsymbol{F}}{\partial \boldsymbol{d}_\Gamma} & \boldsymbol{I} - \frac{\partial \boldsymbol{F}}{\partial \boldsymbol{f}_\Gamma} \end{bmatrix} \begin{bmatrix} \Delta \boldsymbol{d}_{\Gamma,k} \\ \Delta \boldsymbol{f}_{\Gamma,k} \end{bmatrix} = - \begin{bmatrix} \boldsymbol{d}_{\Gamma,k} - \boldsymbol{S}\left(\boldsymbol{f}_{\Gamma,k}\right) \\ \boldsymbol{f}_{\Gamma,k} - \boldsymbol{F}\left(\boldsymbol{d}_{\Gamma,k}\right) \end{bmatrix} \tag{12}$$

$\Delta \boldsymbol{d}_{\Gamma,k} = \boldsymbol{d}_{\Gamma,k+1} - \boldsymbol{d}_{\Gamma,k}$, where k is the current block-Newton coupling iterate. To solve the block-Newton problem requires the computation of the various derivatives of the two field solvers with respect to the interface boundary conditions. Since we are dealing with 'black-box' field solvers obtaining these field quantity sensitivities directly is not possible.

One alternative is to construct approximations to the vector product of the interface Jacobian via finite differencing (see for example [8]). It has however been demonstrated that these gradients are sensitive to the choice of the finite difference step size. Furthermore, approximating the gradients in this fashion requires additional field solver calls which further reduce the overall efficiency of the suggested coupling scheme.

The IBQN-LS method approximates the interface Jacobian in (12) via reduced order models (ROMs), where the ROMs are constructed using the interface information provided by field solvers during the block-Newton coupling iterations.

Assume that k coupling iterations have been performed, therefore the fluid solver has been called k times. Then we have k corresponding interface displacements $\boldsymbol{d}_i^F$ for $i = 1, 2, ...k$ and k corresponding interface tractions $\boldsymbol{f}_i^F$ for $i = 1, 2, ..., k$. With the given observations we can construct two observation matrices. The first observation matrix is associated with historical displacement vectors

$$\boldsymbol{V} = \begin{bmatrix} \Delta d_{1,1}^F & \Delta d_{2,1}^F & ... & \Delta d_{k-1,1}^F \\ \vdots & \ddots & \dots & \vdots \\ \Delta d_{1,N}^F & \cdots & \cdots & \Delta d_{k-1,N}^F \end{bmatrix} \tag{13}$$

where N is the number of degrees of freedom (DOF) along the interface, and $\Delta \boldsymbol{d}_j^F = \boldsymbol{d}_j^F - \boldsymbol{d}_k^F$ for $j = 1, 2, ..., k-1$. Similarly for interface traction observations

$$\boldsymbol{W} = \left[\Delta \boldsymbol{f}_1^F, ..., \Delta \boldsymbol{f}_j^F, ..., \Delta \boldsymbol{f}_{k-1}^F\right] \tag{14}$$

where $\Delta \boldsymbol{f}_j^F = \boldsymbol{f}_j^F - \boldsymbol{f}_k^F$ for $j = 1, 2, ..., k-1$. An approximation of the interface displacement $\Delta \boldsymbol{d}^F$ can then be generated via the linear combination of previous observations:

$$\Delta \boldsymbol{d}^F \approx \boldsymbol{V}\boldsymbol{\alpha} \tag{15}$$

and the change in interface tractions can be approximated as

$$\Delta \boldsymbol{f}^F \approx \boldsymbol{W}\boldsymbol{\alpha}. \tag{16}$$

Via least squares we can then make the following approximation:

$$\boldsymbol{\alpha} = \left(\boldsymbol{V}^T\boldsymbol{V}\right)^{-1}\boldsymbol{V}^T\Delta \boldsymbol{d}^F \tag{17}$$

$$\Delta \boldsymbol{f}^F \approx \boldsymbol{W}\left(\boldsymbol{V}^T\boldsymbol{V}\right)^{-1}\boldsymbol{V}^T\Delta \boldsymbol{d}^F. \tag{18}$$

Equation (18) can be used to approximate the total derivative of the fluid field solver with respect to the interface displacement, i.e.

$$\widehat{\frac{\partial \boldsymbol{F}_k}{\partial \boldsymbol{d}_\Gamma}} = \boldsymbol{W}\left(\boldsymbol{V}^T\boldsymbol{V}\right)^{-1}\boldsymbol{V}^T. \tag{19}$$

It is now possible to obtain an estimate of the interface force $\hat{\boldsymbol{f}}$ given a displacement guess $\hat{\boldsymbol{d}}$,

$$\hat{\boldsymbol{f}} = \boldsymbol{f}_k^F + \widehat{\frac{\partial \boldsymbol{F}_k}{\partial \boldsymbol{d}_\Gamma}}\left(\hat{\boldsymbol{d}} - \boldsymbol{d}_k^F\right). \tag{20}$$

In a similar fashion, we can construct a ROM of the solid solver, such that, given an interface traction guess the ROM provides a corresponding interface displacement guess:

$$\hat{\boldsymbol{d}} = \boldsymbol{d}_l^S + \widehat{\frac{\partial \boldsymbol{S}_l}{\partial \boldsymbol{f}_\Gamma}}\left(\hat{\boldsymbol{f}} - \boldsymbol{f}_l^S\right) \tag{21}$$

where once again

$$\widehat{\frac{\partial \boldsymbol{S}_l}{\partial \boldsymbol{f}_\Gamma}} = \boldsymbol{G}\left(\boldsymbol{Z}^T\boldsymbol{Z}\right)^{-1}\boldsymbol{Z}^T, \tag{22}$$

with $\boldsymbol{G}$ and $\boldsymbol{Z}$ being the corresponding observation matrices associated with the interface for l structural solver calls.

It is important to note that we use different iteration counters k and l because the ROMs are constructed out of sync. It is also not necessary that an equal number of solid and fluid solver calls need to be performed during each coupling iteration.

Using the approximate sensitivities in (19) and (22) the block-Newton linear system outlined in (12) can be expressed as:

$$\left(\boldsymbol{I} - \widehat{\frac{\partial \boldsymbol{S}_l}{\partial \boldsymbol{f}}}\widehat{\frac{\partial \boldsymbol{F}_k}{\partial \boldsymbol{d}}}\right)\Delta \boldsymbol{d}^k = -\left(\boldsymbol{d}_k^F - \boldsymbol{d}_l^S\right) - \widehat{\frac{\partial \boldsymbol{S}_l}{\partial \boldsymbol{f}}}\left(\boldsymbol{f}_l^S - \boldsymbol{f}_k^F\right) \tag{23}$$

$$\left(\boldsymbol{I} - \widehat{\frac{\partial \boldsymbol{F}_k}{\partial \boldsymbol{d}}}\widehat{\frac{\partial \boldsymbol{S}_l}{\partial \boldsymbol{f}}}\right)\Delta \boldsymbol{f}^k = -\left(\boldsymbol{f}_l^S - \boldsymbol{f}_k^F\right) - \widehat{\frac{\partial \boldsymbol{F}_k}{\partial \boldsymbol{d}}}\left(\boldsymbol{d}_k^F - \boldsymbol{d}_l^S\right). \tag{24}$$

An alternative derivation is to combine the two ROMs in (20) and (21) to form the following approximate block-Newton linear system:

$$\left(\boldsymbol{I}-\widehat{\frac{\partial \boldsymbol{S}_l}{\partial \boldsymbol{f}}}\widehat{\frac{\partial \boldsymbol{F}_k}{\partial \boldsymbol{d}}}\right)\hat{\boldsymbol{d}}=\boldsymbol{d}_l^S+\widehat{\frac{\partial \boldsymbol{S}_l}{\partial \boldsymbol{f}}}\left(\boldsymbol{f}_k^F-\boldsymbol{f}_l^S-\widehat{\frac{\partial \boldsymbol{F}_k}{\partial \boldsymbol{d}}}\boldsymbol{d}_k^F\right) \tag{25}$$

$$\left(\boldsymbol{I}-\widehat{\frac{\partial \boldsymbol{F}_k}{\partial \boldsymbol{d}}}\widehat{\frac{\partial \boldsymbol{S}_l}{\partial \boldsymbol{f}}}\right)\hat{\boldsymbol{f}}=\boldsymbol{f}_k^F+\widehat{\frac{\partial \boldsymbol{F}_k}{\partial \boldsymbol{d}}}\left(\boldsymbol{d}_l^S-\boldsymbol{d}_k^F-\widehat{\frac{\partial \boldsymbol{S}_l}{\partial \boldsymbol{f}}}\boldsymbol{f}_l^S\right). \tag{26}$$

While the two sets of approximate linear systems are mathematically equivalent, the approximate system described in (23) and (24) can easily be implemented in a matrix free implementation, and it is the version used in this paper.

In [2] Degroote et al. demonstrated that the performance of IBQN-LS can be significantly improved by retaining information from preceding time steps. Assuming that q previous time steps have been performed, the observations matrix $\boldsymbol{V}^k$ can be defined as:

$$\boldsymbol{V}^k=\left[{}^{n+1}\boldsymbol{V}^k,{}^{n}\boldsymbol{V},...,{}^{n-q+2}\boldsymbol{V},{}^{n-q+1}\boldsymbol{V}\right] \tag{27}$$

where ${}^{n+1}\boldsymbol{V}^k$ is the current time step observation matrix defined by (13) and ${}^{n-i+1}\boldsymbol{V}$ for $i=1,2..q-1$ are the observation matrices at convergence in time step i. We similarly retain histories for all observation matrices $\boldsymbol{W}$, $\boldsymbol{G}$ and $\boldsymbol{Z}$.

To summarize the order of the IBQN-LS coupling scheme:

1) At least two solver calls per ROM is required (necessary for the least squares matrices to have information)
   a) Use fixed relaxation as in (8) for the first iterations until $k\geq 2$ and $l\geq 2$, or the number of retained histories $q>0$.
2) Estimated interface displacement $\rightarrow$ Fluid solver call $\rightarrow$ Interface tractions
   a) Update fluid ROM observation matrices $\boldsymbol{W}$ and $\boldsymbol{V}$ $(k=k+1)$.
3) Solve fluid ROM (24) or (26) $\rightarrow$ estimated interface tractions
4) Estimated interface tractions $\rightarrow$ Solid solver call $\rightarrow$ interface displacements
   a) Update solid ROM observation matrices $\boldsymbol{G}$ and $\boldsymbol{Z}$ $(l=l+1)$.
5) Solve solid ROM (23) or (25) $\rightarrow$ estimated interface displacement.
6) Return to 2, until convergence of interface displacement and/or convergence of interface traction forces.

D. IBQN-POD

In several publications Degroote et al. [2]–[4] have demonstrated that the number of time histories q to retain for the construction of the IBQN-LS observation matrices in (27) is problem dependent. This is certainly true for problem classes where the interface response is relatively simple (e.g. a 1D problem with near constant boundary velocity) or where the interface response is near linear. For this class of problems, the interface Jacobian can be approximated well by retaining only the q newest observation matrices in time.

There is however an equally large number of problems where the interface response is a complex, non-linear behaviour. For this class of problems it becomes beneficial to retain more histories in time, which in turn improves the interface Jacobian approximations. Unfortunately, increasing the number of retained history vectors in (27) leads to the potential of the solution matrices $\left(\boldsymbol{I}-\widehat{\frac{\partial \boldsymbol{S}_l}{\partial f}}\widehat{\frac{\partial \boldsymbol{F}_k}{\partial d}}\right)$ and $\left(\boldsymbol{I}-\widehat{\frac{\partial \boldsymbol{F}_k}{\partial d}}\widehat{\frac{\partial \boldsymbol{S}_l}{\partial f}}\right)$ becoming increasingly ill-conditioned.

The ill-conditioning is related to the close proximity of one or more of the LS observation vectors. As such there is a problem specific optimal choice for the number of history vectors to retain. As we will demonstrate in Section III, if q is chosen to be too large then the convergence properties deteriorate due to increasing ill-conditioning, if convergence does not fail altogether. Conversely, if q is chosen to be too small then a lot of valuable information is discarded and sub-optimal convergence rates are once again achieved.

For this reason, we suggest a minor augmentation to the IBQN-LS based on proper orthogonal decomposition (POD). POD provably forms the optimal linear decomposition of any given set of system observations. It therefore allows for a mathematically quantifiable way in which to truncate the observation matrices such that they essentially retain 'all' the information while limiting the extent of ill-conditioning.

To facilitate the discussion on the POD augmentation, we start with the 'method of snapshots', a solution method introduced by Sirovich [9]. The method of snapshots is a truncated solution procedure to solve for the POD basis functions for a non-square observation matrix. Consider the observation matrix $\boldsymbol{V}$ which is of size $M\times N$ where M is the number of observation vectors and N is the DOF of the system (for the FSI problem, this would be the number of DOFs along the interface boundary). The method of snapshots requires the solution of the eigenvalue problem of an $M\times M$ autocorrelation matrix of the form:

$$\boldsymbol{R}=\frac{1}{M}\boldsymbol{V}\boldsymbol{V}^T, \tag{28}$$

where the eigenvectors $\boldsymbol{a}$ of $\boldsymbol{R}$ are computed as an intermediate step to computing the basis modes, i.e.

$$\boldsymbol{R}\boldsymbol{a}=\boldsymbol{\lambda}\boldsymbol{a}, \tag{29}$$

where the POD basis modes $\boldsymbol{\varphi}$ are then computed as the linear combination

$$\boldsymbol{\varphi}=\boldsymbol{a}\boldsymbol{V}. \tag{30}$$

The eigenvalues λ_i in (29) provide an indication as to how much of the system information is contained in the corresponding POD modes $\boldsymbol{\varphi}_i$. Therefore by ordering the eigenmodes $\boldsymbol{\varphi_i}$ based on the ranked eigenvalues (from largest to smallest), it is possible to truncate the system to only the c most dominant basis modes:

$$\widehat{\boldsymbol{x}}^k \approx \sum_{i=1}^{c} \alpha_i^k \boldsymbol{\varphi_i} \tag{31}$$

where c is the number of retained basis modes, $\widehat{\boldsymbol{x}}^k$ is an approximation of the k^{th} vector of the observation matrix $\boldsymbol{V}$ and $\boldsymbol{\alpha}_i$ is the i^{th} eigenvector of $\boldsymbol{a}$.

Let us now return to the approximations in (15) and (16). Using the newly computed basis modes for $\boldsymbol{V}$, we replace (15) with

$$\Delta \boldsymbol{d}^F \approx \boldsymbol{\varphi} \boldsymbol{\alpha}_{\text{POD}} \tag{32}$$

and using least squares we solve for $\boldsymbol{\alpha}_{\text{POD}}$ such that

$$\boldsymbol{\alpha}_{\text{POD}} = \left(\boldsymbol{\varphi}^T \boldsymbol{\varphi}\right)^{-1} \boldsymbol{\varphi}^T \Delta \boldsymbol{d}^F. \tag{33}$$

Furthermore, the POD expansion coefficients $\boldsymbol{\alpha}_{\text{POD}}$ can be related as a linear combination to the eigenvectors $\boldsymbol{a}$. As such, we obtain a new approximation for (16):

$$\Delta \boldsymbol{f}^F \approx \boldsymbol{W} \boldsymbol{a} \left[\left(\boldsymbol{\varphi}^T \boldsymbol{\varphi}\right)^{-1} \boldsymbol{\varphi}^T \Delta \boldsymbol{d}^F\right]. \tag{34}$$

We now have the ability to truncate both $\boldsymbol{a}$ and $\boldsymbol{\varphi}$ in accordance to the ranked eigenvalues λ. By retaining only the c most dominant modes, the condition number of the least squares solution in (33) of $\left(\boldsymbol{\varphi}^T \boldsymbol{\varphi}\right)^{-1} \boldsymbol{\varphi}^T$ is then provably equal to $\sqrt{\frac{\lambda_1}{\lambda_c}}$. We therefore have strong control over the condition number of the least square matrices, which in turn limit the condition number of the interface system matrices $\left(\boldsymbol{I} - \frac{\widehat{\partial \boldsymbol{S}_l}}{\partial f} \frac{\widehat{\partial \boldsymbol{F}_k}}{\partial d}\right)$ and $\left(\boldsymbol{I} - \frac{\widehat{\partial \boldsymbol{F}_k}}{\partial d} \frac{\widehat{\partial \boldsymbol{S}_l}}{\partial f}\right)$.

We do the same for the Solid ROM, and with the new POD based approximations reconstruct the approximate interface Jacobian in (23)-(24).

It should be noted that the dominant additional cost of the proposed IBQN-POD model is the solution of an $M \times M$ eigenvalue problem and the construction of the covariance matrix $\boldsymbol{R}$ with associated cost $N \times M^2$. Although in typical problems $M \ll N$, it should be noted that if a large number of historical observations are retained that M can quickly grow to a non-trivial value. In such a scenario it might be advisable to solve the eigenvalue problem using an iterative algorithm solving for only the c most dominant eigenvalues and eigenvectors.

III. Results

The test case considered here is the 3D simulation of flow through a straight flexible tube presented in [10] and is representative of the type of problems encountered in hemodynamics. The tube has a length of 5cm, an inner radius of $r_i = 0.5$cm and outer radius of $r_o = 0.6$cm. The structural density is $\rho_s = 1.2\text{g/cm}^3$ with a Young's modulus and Poisson's ratio of $E = 3 \times 10^4\text{dyne/cm}^2$ and $\nu_s = 0.3$ respectively. In this paper we make use of a hyperelastic Neo-Hookean material property as opposed to a linear elastic model used to analyse the IBQN-LS and its many variants in previous publications [2]–[4]. Using a Hyperelastic material property increases the non-linear response of the solid field solver which in turn significantly complicates the construction and performance of the IBQN-LS approximate interface Jacobian. The fluid domain is modelled with a viscosity of $\mu = 0.03$ Poise and density of $\rho_f = 1.0\text{g/cm}^3$. The time step size is $\Delta t = 0.0001$s.

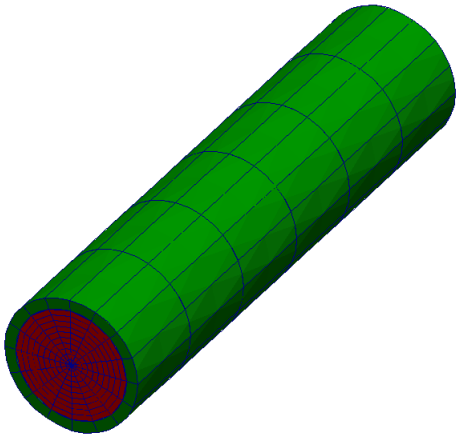

Fig. 1. Flexible tube benchmark problem with the employed fluid (red, 1600 hexahedral finite volume elements) and solid (green, 96 twenty node quadratic brick finite element) computational grids.

The tube is fixed at both ends and the fluid and structural domains are initially at rest. A traction of $1.3332 \times 10^4\text{dyne/cm}^2$ is applied for 3×10^{-3}s which results in a pressure wave propagating through the length of the tube. The fluid flow and deformation of the tube at time steps 0.002, 0.0055 and 0.008 seconds is shown in Figure 2 for 10 times enlarged structural deformation.

The structural and fluid field solvers employed for this problem are the open-source solvers Calculix and OpenFOAM. 1600 eight node hexahedral finite-volume elements and 96 twenty node quadratic brick finite elements are employed for each of the respective domains. The time step iteration convergence tolerance used for this test problem is

$$\frac{\left|\boldsymbol{d}_{\Gamma,i+1}^{n+1} - \boldsymbol{d}_{\Gamma,i}^{n+1}\right|}{\sqrt{N}} \leq 10^{-7} \tag{35}$$

The $\sqrt{N}$ is included to remove the dependency of the solution residual to the interface mesh size, where N is the DOF of the interface.

We run the problem for a total of 100 time steps, which is approximately the time required for the pressure pulse to propagate through the length of the tube. In Figure 3 we compare the number of coupling iterations required by the three iteration schemes, namely Aitken's Δ^2, IBQN-LS where the values in the brackets $(\cdot)$ indicate the number of retained histories in time and the IBQN-POD where all the histories are retained. The average number of iterations are summarized in Table I.

TABLE I
SUMMARY OF THE AVERAGE NUMBER OF REQUIRED COUPLING ITERATIONS. QUANTITIES IN BRACKETS $(\cdot)$ INDICATE NUMBER OF RETAINED HISTORIES

Coupling Scheme	Avg. number of iterations
Aitken's Δ^2	29.09
IBQN-LS(All)	8.32 (non-convergence time step 84)
IBQN-LS(5)	6.95
IBQN-LS(15)	5.26
IBQN-POD(All)	3.31

For Aitken's relaxation, we make use of an approximation of the boundary position at the start of each new time step. The approximation is based on the interpolation of converged interface position from two previous time steps [2]

$$\boldsymbol{d}_0^{n+1} = \frac{5}{2}\boldsymbol{d}^n - 2\boldsymbol{d}^{n-1} + \frac{1}{2}\boldsymbol{d}^{n-2}. \tag{36}$$

While fixed point iteration schemes benefit from a good initial guess we have observed that the block-Newton methods investigated in this paper gain little to no improvement in the coupling iterations by employing the interpolated approximation. Therefore, to remove any ambiguity when comparing the coupling performance of the block-Newton methods we start each new time step with the initial condition equal to the converged displacement from the previous time step

$$\boldsymbol{d}_0^{n+1} = \boldsymbol{d}^n. \tag{37}$$

Upon comparing the results in Table I and Figure 3 it becomes apparent that Aitken's dynamic relaxation method is somewhat ill-suited to the problem. While convergence is attained, the number of coupling iterations, and hence field solver calls, is significantly higher than the results of the approximate block-Newton methods.

If we now analyse the behaviour of the IBQN-LS algorithm, the dependence on the number of retained histories in time q becomes apparent. In Figure 4 a comparison of the condition number of $\left(\boldsymbol{I} - \widehat{\frac{\partial \boldsymbol{F}_k}{\partial \boldsymbol{d}}}\widehat{\frac{\partial \boldsymbol{S}_l}{\partial \boldsymbol{f}}}\right)$ is provided as a function of the iteration count. By retaining too many histories, the solution matrices for the IBQN-LS approximations become ill-conditioned which in turn causes the coupling scheme to struggle and eventually lead to non-convergence. On the contrary retaining too few histories, while resulting in a well-conditioned system, looses valuable system information. The optimal q for this current problem is approximately 15.

For the IBQN-POD coupling scheme, we selected the c most dominant modes based on the criteria of the ratio of maximum to minimum eigenvalues

$$\frac{\lambda_1}{\lambda_c} \leq 10^{11}, \tag{38}$$

which leads to a maximum condition number for the LS matrices in (33) of 3.16×10^5. The approximate interface approximations therefore remain well-conditioned throughout the simulation while essentially retaining all the system information. The behaviour of the IBQN-POD is therefore more

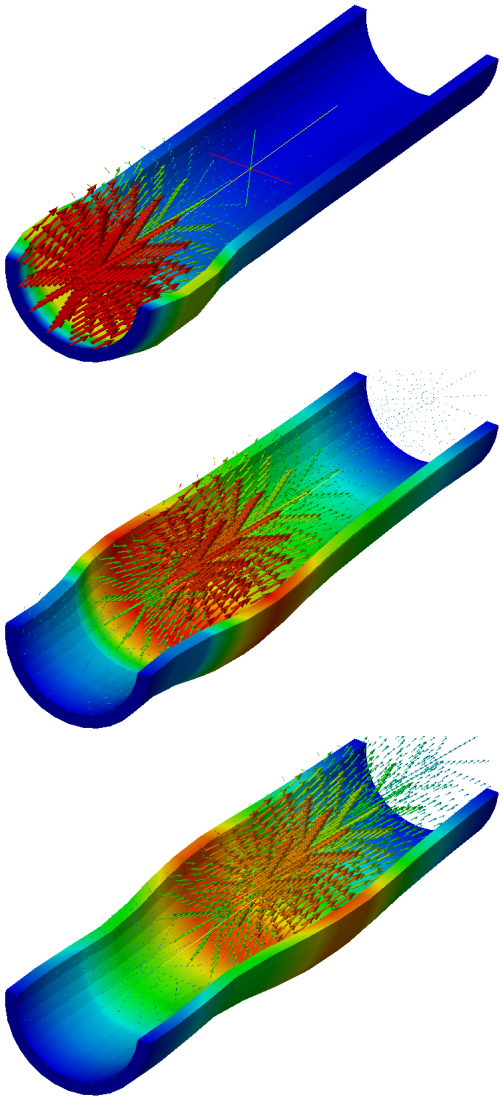

Fig. 2. Pressure wave propagation plots at time step 0.002, 0.0055 and 0.008 seconds. Structural displacement magnified 10 times. Colour fields represent the pressure (for the fluid flow) and displacement magnitude of the tube wall.

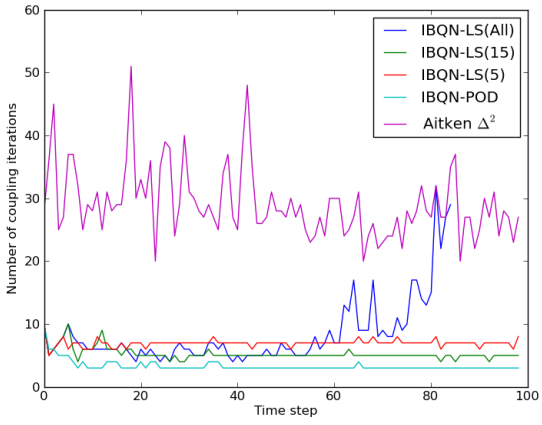

Fig. 3. Comparison of the number of solver coupling iterations.

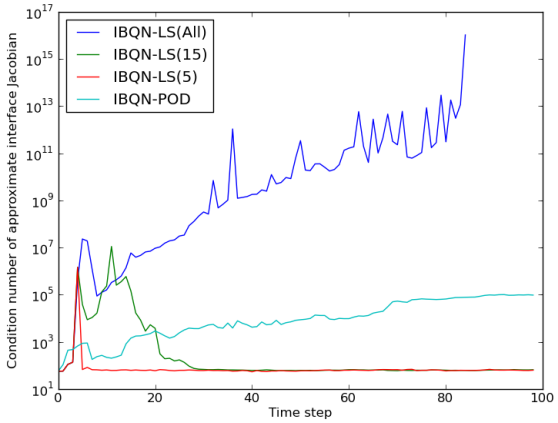

Fig. 4. Condition number of the approximate interface Jacobian matrix

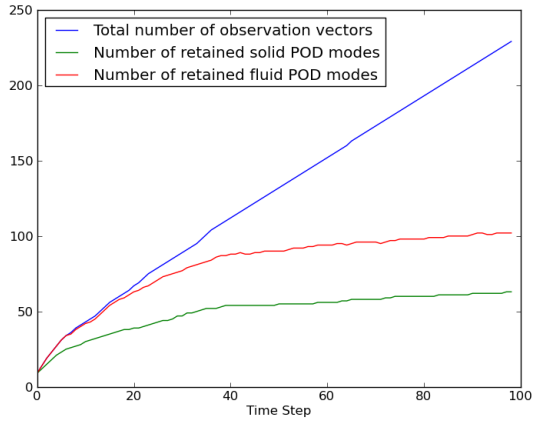

Fig. 6. Comparison of the number of retained POD modes for the solid and fluid ROMs compared to the total number of observation vectors

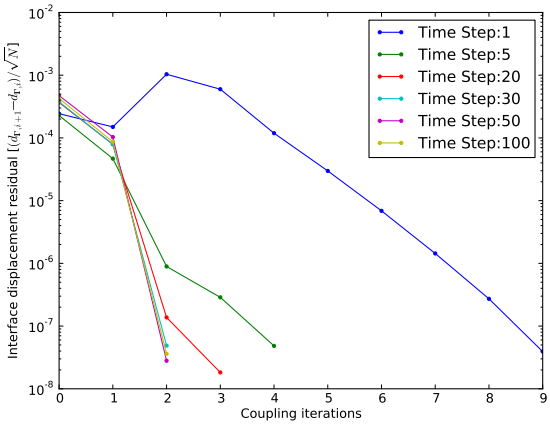

Fig. 5. Block-Newton coupling iteration convergence rates for IBQN-POD coupling scheme.

predictable and the benefit of retaining all the histories is highlighted in Figure 5, which illustrates the convergence rates at 6 selected time steps. As more information is captured by the system observation matrices the convergence rates continue to improve, where from time step 20 onwards the convergence rates are near quadratic.

A plot of the total number of retained history vectors along with the number of retained POD modes for the solid and fluid ROMs is shown in Figure 6. For both the fluid and solid POD ROMs, the number of retained modes is far fewer than the total number of retained observation vectors. This highlights the extent of duplicated information within the respective observation matrices and hence why ill-conditioning becomes an issue.

The major limitation thus of the proposed POD augmentation is the necessity to retain all history vectors. For the current flexible tube problem this is not a problem as the total number of retained history vectors remain small. If however the problem requires a large number of time steps to run to completion the numerical effort required to maintain the full set of history vectors may become excessive. An important factor to consider thus is the efficiency gained by the retention of more histories as a function of the increased numerical effort. This will be the focus of future work along with using the available subspace information to predict which histories can safely be rejected without sacrificing the combined information that is retained.

IV. Conclusion

In this paper we have outlined an augmentation to the original IBQN-LS approximate block-Newton FSI strong coupling scheme via the use of proper orthogonal decomposition. The performance of the original IBQN-LS method is strongly governed by the number of previous time step histories that are retained, where the optimal choice is problem specific. Maintaining too few historical observation results in sub-optimal convergence rates, whereas retaining too many results in increasingly ill-conditioned least squares matrices which can lead to non-convergence.

The POD augmentation allows for the re-use of all observations from previous time steps by limiting the matrix ill-conditioning. Retaining all histories improves the approximation of the interface block-Newton Jacobian, which in turn improves the coupling iterations' convergence rates. Once sufficient information has been captured, the IBQN-POD interface ROM can produce near quadratic convergence rates.

The major limitation of the proposed augmentation is the necessity to retain all previous history vectors which may lead to a compromise in the computational cost of the simulation. Future work will therefore focus on using the ROM subspace information already available to determine which of the previous time step histories can be safely removed while limiting the loss of information.

References

[1] J. Vierendeels, L. Lanoye, J. Degroote, and P. Verdonck, "Implicit coupling of partitioned fluid-structure interaction problems with reduced order models," *Computers and Structures*, vol. 85, pp. 970–976, 2007.

[2] J. Degroote, R. Haelterman, S. Annerel, P. Bruggerman, and J. Vierendeels, "Performance of partitioned procedures in fluid-structure interaction," *Computers and Structures*, vol. 88, pp. 446–457, 2010.
[3] J. Degroote, A. Swillens, P. BruggerMan, R. Haelterman, P. Segers, and J. Vierendeels, "Simulation of fluid-structure interaction with the interface artifical compressibbility method," *International Journal for Numerical Methods in Biomedical Engineering*, vol. 26, pp. 276–289, 2010.
[4] J. Degroote, K. Bathe, and J. Vierendeels, "Performance of a new partitioned procedure versus a monolithic procedure in fluid-structure interaction," *Computers & Structures*, vol. 87, no. 11-12, pp. 793–801, 2009.
[5] C. Förster, W. Wall, and E. Ramm, "Artificial added mass instabilities in sequential staggered coupling of nonlinear structures and incompressible viscous flows," *Computer Methods in Applied Mechanics and Engineering*, vol. 196, no. 7, pp. 1278–1293, 2007.
[6] P. Causin, J. Gerbeau, and F. Nobile, "Added-mass effect in the design of partitioned algorithms for fluid–structure problems," *Computer methods in applied mechanics and engineering*, vol. 194, no. 42, pp. 4506–4527, 2005.
[7] U. Küttler and W. Wall, "Fixed-point fluid–structure interaction solvers with dynamic relaxation," *Computational Mechanics*, vol. 43, no. 1, pp. 61–72, 2008.
[8] H. Matthies and J. Steindorf, "Partitioned strong coupling algorithms for fluid–structure interaction," *Computers & structures*, vol. 81, no. 8, pp. 805–812, 2003.
[9] L. Sirovich, "Turbulence and the dynamics of coherent structures. part i: Coherent structures," *Quarterly of applied mathematics*, vol. 45, no. 3, pp. 561–571, 1987.
[10] U. Kuttler, M. Gee, C. Forster, A. Comerford, and W. Wall, "Coupling strategies for biomedical fluid-structure interaction problems," *International Journal for Numerical Methods in Biomedical Engineering*, vol. 26, pp. 305–321, 2010.